Defected Ground Structure Microstrip Patch Antenna Design for Radio Frequency identification (RFID) and Wireless Communications

Muhammad Azeem Aslam[1], Hina Maryam[2]

[1]Department of Physics, University of Okara, Okara, Pakistan

[2]Department of Physics, University of Okara, Okara, Pakistan

Abstract

The future of wireless communications such as WLAN (IEEE 802.11ah), radio frequency identification (RFID), wireless sensor networks, structure health monitoring, and home automation will integrate defected ground structure (DGS) antennas. The proposed design having defected ground structure (DGS) antenna design suited for RFID and wireless system operation. Working at 1.96 GHz, this DGS antenna has an exceptional return loss of -31 dB against antenna I which is having frequency of 1.93 GHz and a return loss of -13 dB. The SAR analysis factor proves its appropriateness for human-friendly. This study supports the feasibility of the antenna for improving the performance and ability of the system with the functioning of the ultra-high frequency (UHF) frequency range with the help of simulation and fabrication.

Keywords

Defected Ground Structure (DGS), Microstrip Patch Antenna, RFID, UHF Frequency Range, Specific Absorption Rate (SAR)

1. Introduction

Defected ground structure antennas are paving the way for wireless communication networks. Simple patch antennas can reduce an antenna's performance by causing unwanted radiation and mutual coupling, while DGS antennas can suppress these surface waves and improve antenna's performance. In today's world, DGS antennas are used for IoT (internet of things) applications [1] and DGS antennas [2] also introduce frequency-selective surface [3]. By introducing defects in the ground, the antenna size can also be reduced for the required frequency range. This paper introduces the design of a microstrip patch antenna to be used for RFID applications [4]. The return loss and VSWR of our antenna are also analyzed which means that there is a small amount of reflection of the signal and good impedance matching, which is crucial for RFID tags communication. Due to the small size and flat configuration of the micro-strip patch antenna, it is ideal for incorporating with different RFID systems used in logistics, inventory and access control. This research reveals defected ground structure (DGS) antenna operating for wireless networks such as wireless local area network (WLAN), radio frequency identification (RFID) and wireless Sensors as shown in Figure 1.The DGS structures come in a variety of geometries, including square [5], circular [6], dumbbell [7], spiral [8],l-shaped [9], concentric ring [10], u-shaped and v-shaped [18-20], hairpin DGS [21] and hexagonal DGS [22].

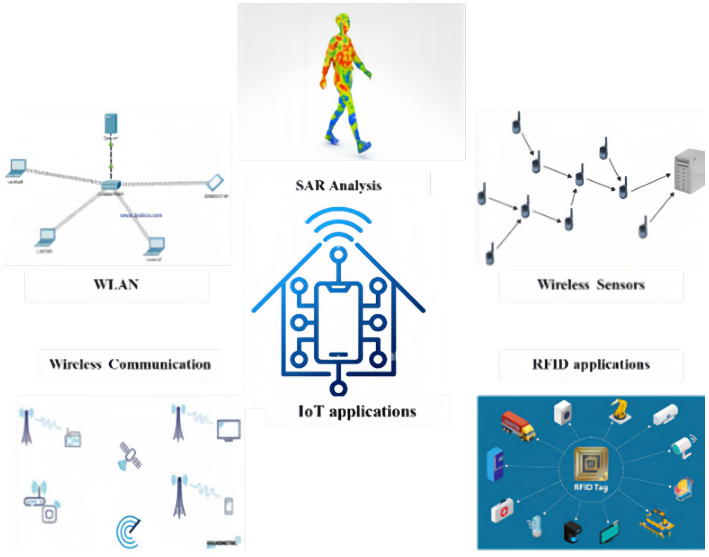

Figure 1. Applications of Proposed Antenna

Those structure are further applied for different applications. DGS are most effective at the filter design of microwaves [6], power amplifiers [10], splitters [11], oscillating microwave devices [12] transmission lines [13], and micro-strip antennas the efficient utilization of the defected ground structure for the above-explained improved metrics is found.

The research objectives encompass two primary domains: The Internet of Things (IoT) and medical imaging. In the situation of wireless communications, the designed antenna V is directed at enhancing of the connectivity, signal quality, and reliability of the whole system over various networking devices. Nevertheless, the antenna V will probably get have various applications in medical imaging systems, namely, designing imaging systems with enhanced diagnostic accuracy, resolution, and performance. Specific Absorption rate (SAR) [14-22] is a useful parameter to be used in medical imaging systems.

In this paper, a defected ground structure antenna is proposed. First, a microstrip patch antenna named as antenna I is simulated and analyzed than number of slots in patches and defects in the ground has been introduced to get the desired frequency range for RFID applications. The antenna V is also tested for SAR calculation. Consequently, a DGS antenna is than fabricated and measured to verify the correction of the proposed method.

2. Antenna Design and Methodology

The process of design begins with electromagnetic analysis of the Antenna I as shown in Figure 2. Thus, the objective is to find the best choice of the dimensions of the microstrip element and Defected Ground Structure (DGS). For the analysis, the patch antenna that initially designed is 21 mm x 22 mm is chosen for the parametric study.

An optimized without defects antenna I is operating at a frequency of 2.73 GHz with a return loss of -14 dB. Antenna II containing one ground defect and three slots in Patch 1 got frequency of 2. 6 GHz of shift with -6 dB return loss. Antenna III makes three improvements to the ground in the form of defects with one slot in Patch 2 and brings frequency of 1.98 GHz with a return loss of -20 dB. In Antenna IV, Ground defects are four and 1 slot in Patch 3, having operating frequency of 1.96 GHz and return loss of -20 dB. Finally, Antenna V go with five ground defects and a slot in Patch 4, showing the best return loss of -31 dB at 1.96 GHz. FR-4 substrate sheets with a relative permittivity of εr=4.4 are carefully chosen and prepared to meet the needed dielectric properties and thickness. The effect of the changes in patch and ground plane on S11 is shown in Figure 7.

The detailed dimensions of the proposed antenna are shown in Figure 3. The Antenna V is having substrate length L=21mm with substrate width W=22mm. The patch is consisted of a T-Shaped structure in which three slots have been inserted to right side and three slots have been inserted to left side of the structure. The dimensions of the patch and ground is taken in millimeters and are given as a=19.85, b=1.5, c=1, d=2, f=15, g=0.9, h=1.75, i=0.5, j=4.5, k=4, l=1.4, m=3.5, n=0.34, o=0.8, p=2.8, q=0.75 and for the path dimensions LP_1=5.5, WP_1=5.5, Lp_2=3, WP_2=3.8, LP_3=3, WP_3=2.5, LP_4=3, WP_4=4. The dimensions of the defects in the ground are given as RC_1=2.75, RC_2=2, DB_x=4.2, DB_y=0.8 and the difference between the defects is RCi=7.

The proposed antenna is then set to measure a specific absorption rate (SAR). Initially, the human body phantom is designed by using the software and then synthesized in laboratory. The phantom consists of three layers: skin, fat, and muscle, respectively. The widths of skin, fat and muscle are 2 mm, 8 mm and 23 mm respectively.

Figure 4 shows the dimensions of the human phantom. Table 1 illustrates the dielectric properties of different human body tissues.

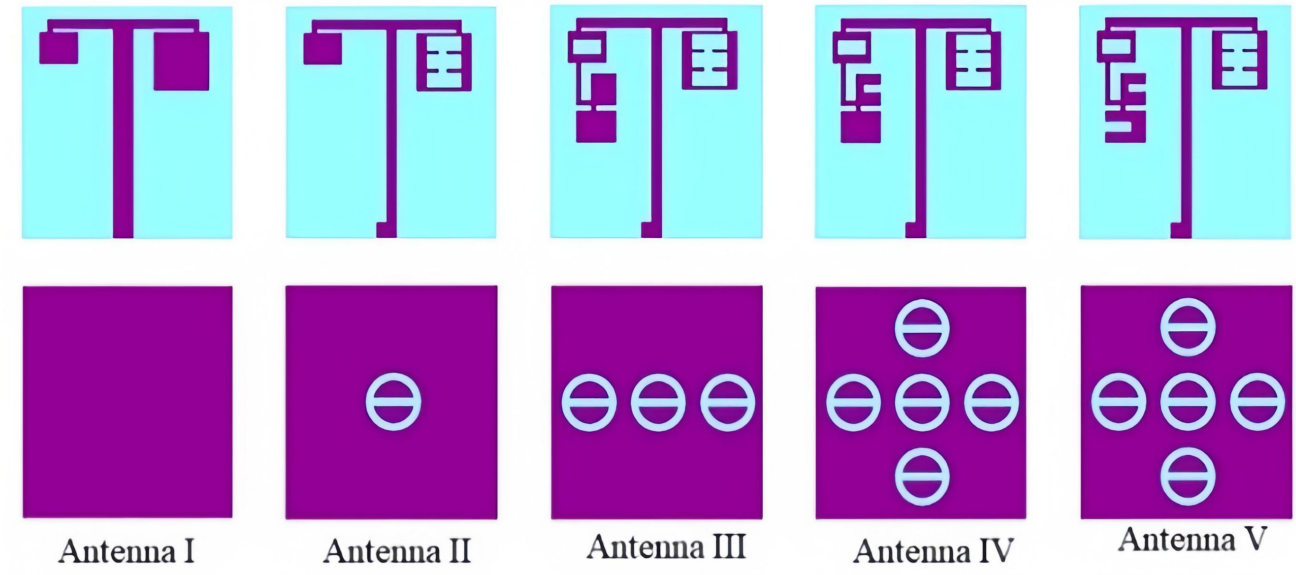

Figure 2. Steps of Proposed Antenna

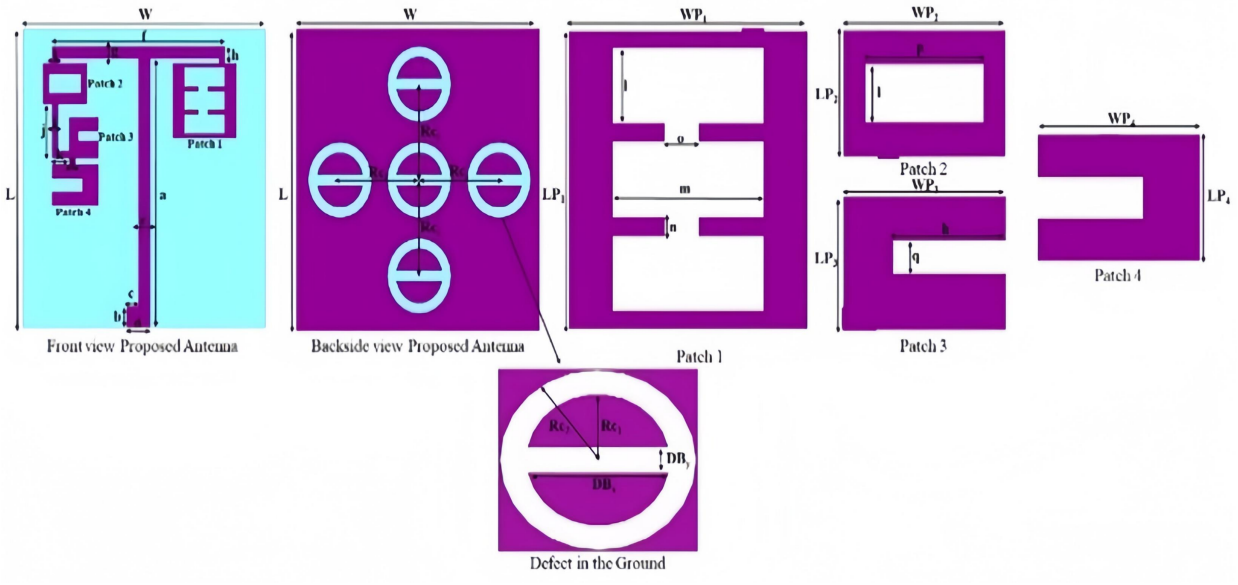

Figure 3. Dimensions of Proposed Antenna

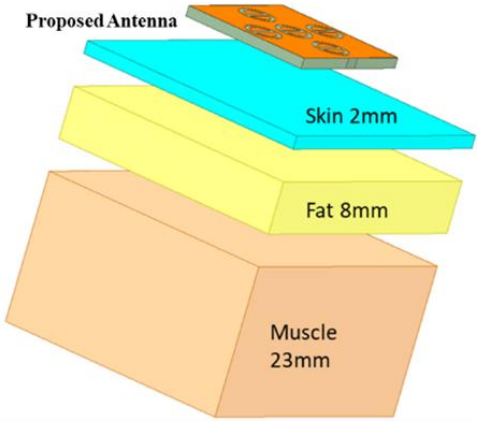

Figure 4. Dimensions of human Phantom

Table 1. Dieletric Properties of Human Body Phantom

Tissues	Permittivity ϵ_r	Conductivity (S/m)	Loss Tangent (tanσ)	Density (Kg/m^3)
Muscle	52.79	1.705	0.24191	1060
Fat	5.28	0.1	0.19382	1100
Skin	31.29	5.0138	0.2835	1100

3. Results and Discussion

The fabricated-designed antenna model, shown in Figure 5, is tested using sophisticated measurement instruments. VNA modal SV6301A with frequency range 1 MHz- 6.3 GHz is configured to correct for calibration factors and generate high accuracy S parameters. At the end, the outcomes come apart and are compared one-to-one. The S11 results for both simulated and fabricated versions shown in Figure 6. Figure 7 shows that the proposed patch antenna (Antenna V) with a defected ground structure (DGS) outperforms the antenna I, which operates at 2.73 GHz with a return loss of -13 dB. The DGS antenna (antenna V), operating at 1.96 GHz, achieves a superior return loss of -31 dB, indicating reduced reflections and better impedance matching. This improvement highlights the DGS's effectiveness in enhancing performance, making the antenna suitable for high-frequency applications like RFID.

After the enhancement of these results, the antenna is then set for parametric analysis. This work presents the S11 results for different widths of feedline and at different radii of the defects on the ground. Figure 8 shows the comparison of these changes in feedline, which shows that the proposed antenna V is radiating well while changing the feed width. It has been observed that the antenna is operating at enhanced return loss.

This work also sheds light on the parametric analysis of defects in the ground. Initially, the inner defect remained the same and the outer defect varied from 2.5-3 mm. After getting these results, the Inner defect varied from 2-2.5 mm and outer defect remained the same. It has been investigated that no change has occurred except enhancement for return loss on the proposed dimensions of patch antenna.

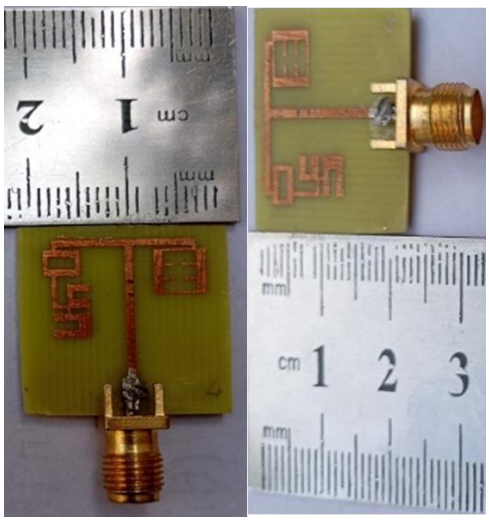

Figure 5. Fabricated Antenna (a) front-side view (b) Back-side view

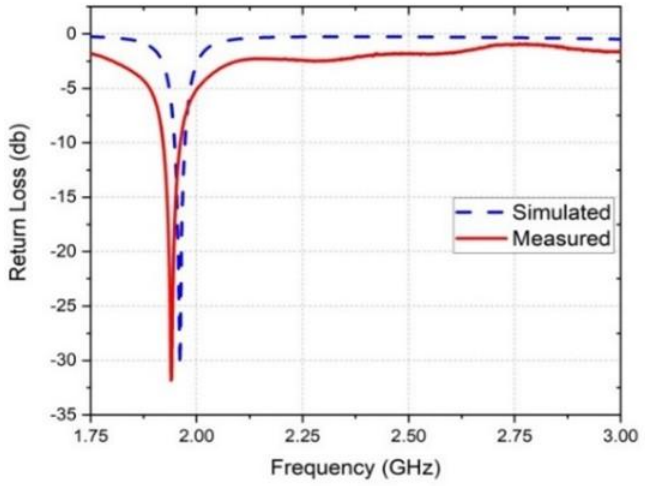

Figure 6. Fabricated and Simulated results of S11 parameters for Antenna V

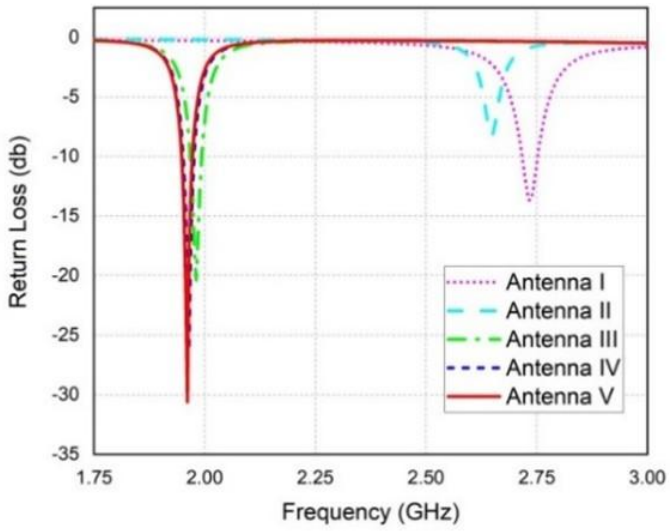

Figure 7. Simulated results of Different steps of Proposed Antenna

As the Antenna V is operating for RFID applications, it is found that placement of Antennas plays a crucial role. For this context, Time delay parameter plays an important role in calculating the efficiency of system. Initially, Time delay factor is calculated by the use of equation as shown in equation.

$$T=2\frac{D^2}{\lambda} \quad (1)$$

Here D is the distance or length between the antennas and λ is the wavelength.

The antennas are placed face to face, Face to Side and Side to Side to measure the time delay factor for each orientation. It is found that the time delay is approximately 1 ns which indicates a very low delay between transmission and reception and minimal signal distortion. The proposed antennas are then fabricated and tested using a vector network analyzer (VNA) for different orientations of antennas. The fabricated antennas are placed on distance of 13mm as calculated by equation 1. It has been observed that for each orientation the value of time domain is acceptable for RFID applications. Results for each orientation is excluded and drawn as shown in Fig. 9 which shows the value of time delay is 1ns.

Figure 10 compares the VSWR of the steps of antennas, i.e., antenna I to antenna V. The VSWR of the proposed antenna, Antenna V, is 1.77, which can shed light on what type of antenna performs better. The VSWR of antenna-I to antenna-IV is 1.9, 2, 2.6 and 2.75 respectively, which shows lack of matching of impedance and signal loss between transmission and reception. The DGS antenna's outstanding VSWR value of 1.77 means the best impedance matching with minimal signal reflection. So, transmission efficiency will be maximized and signal fidelity will be increased.

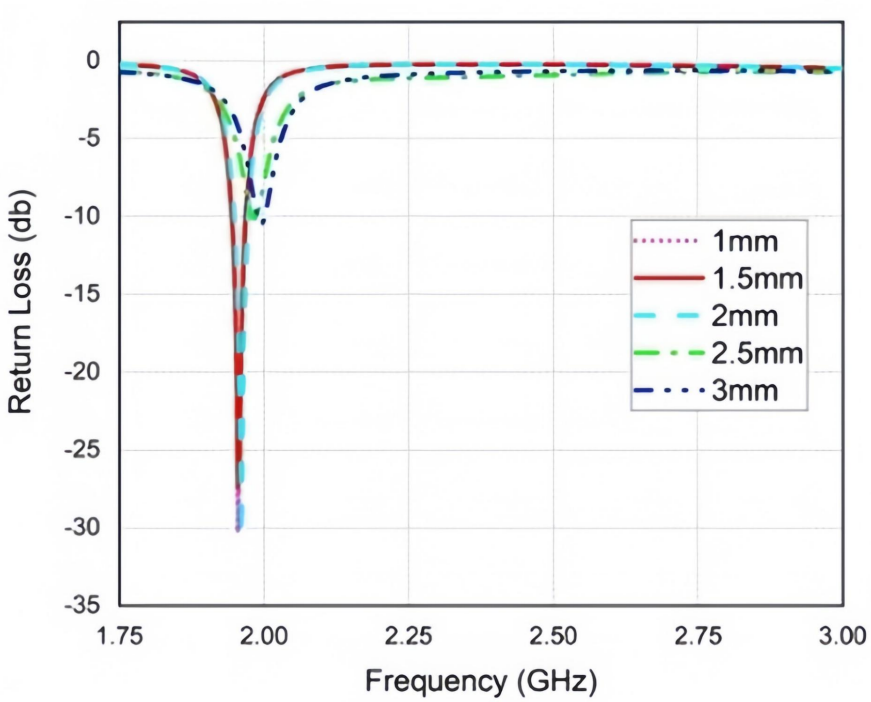

Figure 8. Parametric Analysis of Feedline

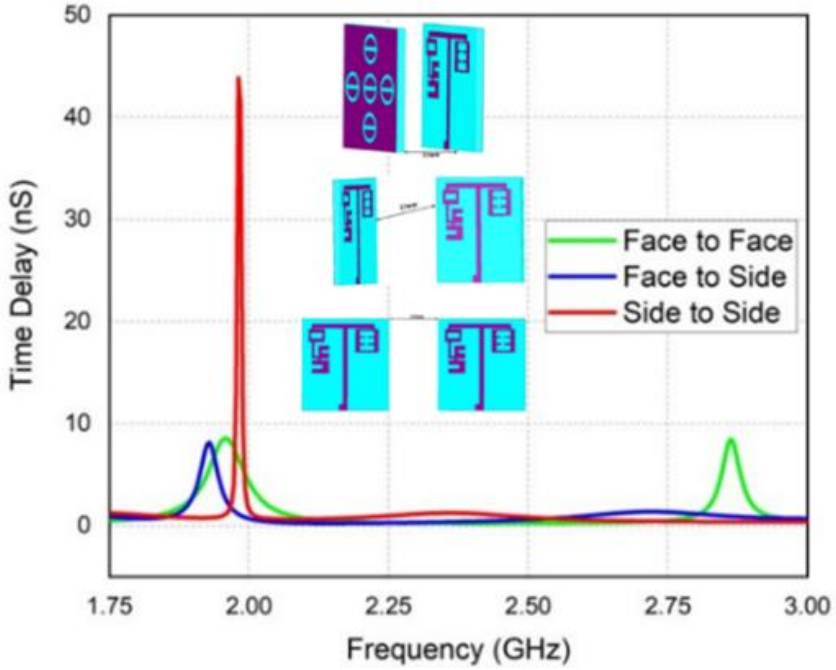

Figure 9. Time Delay for different orientations of faricated antennas

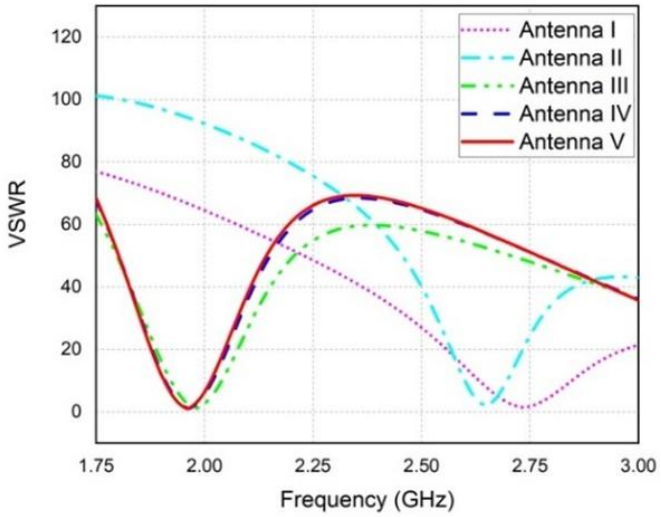

Figure 10. VSWR for different Steps of Antennas

To comprehensively assess the human health effect of this wireless power transfer system, Figure 11 details the specific absorption rate (SAR). SAR can be calculated by using the following mathematical equation:

$$SAR=\frac{\sigma E2}{\rho} \quad (2)$$

Here σ is the conductivity of the tissue measured in siemen/meter (S/m), E is the root mean square of the induced electric field measured in volt/meter (V/m) and ρ is the density of the tissue measured in kilogram/meter^3 (Kg/m^3)

The experiment shows the specific absorption rates of 37 W/kg (for on-body exposure) as shown in Figure 11. This suggests the feasibility of SAR in different scenarios because it also gives forethought to the safety of wireless communication devices, especially their usage near body.

The Proposed Antenna design is then compared to the literature as shown in Table 2. It has been observed that the antenna is small in size and effecting less to human body because it has low value of specific absorption rate than the designs discussed in the literature. The fabricated antenna is then placed on surface and inside a human body phantom as shown in Figure 11. The research reveals that the antenna is performing well in every aspect. The results of fabricated antenna are then tested using different methods, i.e., in the air, on the surface of a human body phantom, and inside a human body phantom. The graphs as shown in Figure 12 reveal the characteristics of the antenna V operating in air at 1.96 GHz with a return loss -32 dB, on surface of a human body phantom at 1.82 GHz return loss -12 dB. When antenna V is placed inside the human body phantom, itoperates on 1.3 GHz at -25 dB.

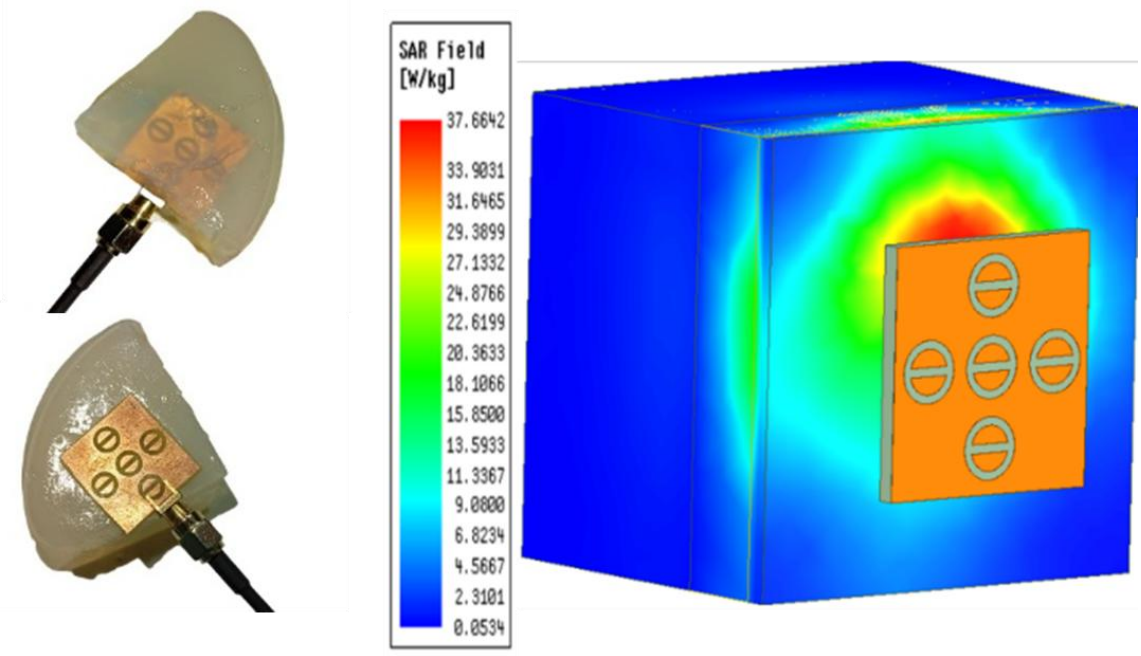

Figure 11. (a) Antenna V on surface and inside of Phantom **(b)** Simulated result of Antenna V on surface of Phantom

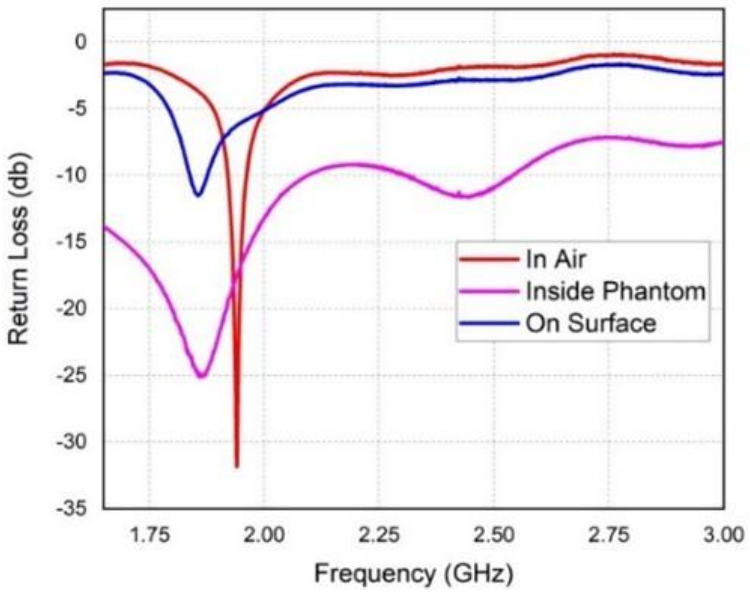

Figure 12. Fabricated results of Antenna V Placed on Phantom at different points

Table 2. Comparison of this Work with Literature

Ref. No	Dimensions (mm^3)	Operating Frequency (GHz)	SAR (W/Kg) @1gm
[17]	(23x16.4x1.27)	0.402	284.5
[18]	(15 × 21.5 × 1.57)	2.45	Not calculated
[19]	(3.14 × 28.6 × 1.3)	0.402/ 2.45	666/ 676
[20]	(3.14 × 23 × 0.634)	2.45	649
[21]	(15 × 15 × 1.27)	0.915	517
[22]	(3.14 × 22.09 × 1.27)	0.915	778
This Work	(21 × 22 × 1.67)	1.96	37

4. Conclusion

It has been concluded that the defected ground structure antenna is suitable for RFID and other wireless communication networks. The design process optimization and strict manufacturing procedures utilized for the antenna's fabrication rendered it a high-performance antenna. Moreover, enriching the outcomes from this study also enriches knowledge in antenna engineering and points the way for advances in the future field of antenna engineering. For the next research move, the approach tagged on with additional enhancements like the UHF operation and further miniaturization techniques can be explored to meet the changing needs of contemporary communication systems. SAR analysis also reveals the efficiency of the proposed antenna. It has been observed through different results that antenna V is suitable for RFID applications and least effected to human bodies. For future endeavors, the antenna will be studied for further advancements in the research field.

References

[1] HUSSAIN, K. and I.-Y. OH, Review of Joint Radar, Communication, and Integration of Beam-forming Technology. 2024.
[2] Khandelwal, M.K., et al., Defected ground structure: fundamentals, analysis, and applications in modern wireless trends. 2017. 2017(1): p. 2018527.
[3] Mamedes, D.F., Design of Frequency-Selective Surfaces for Advanced Applications. 2024, University of Victoria.
[4] Marrocco, G.J.I.t.o.a. and propagation, RFID antennas for the UHF remote monitoring of human subjects. 2007. 55(6): p. 1862-1870.
[5] Colaco, J. and R. Lohani. Multi-band Microstrip Square Patch Antenna Design for IoT based RFID technology and its various applications. in 2021 6th International Conference for Convergence in Technology (I2CT). 2021. IEEE.
[6] Er-Rebyiy, R., et al. A new design of a miniature microstrip patch antenna using defected ground structure DGS. in 2017 International Conference on Wireless Technologies, Embedded and Intelligent Systems (WITS). 2017. IEEE.
[7] Chakraborty, S., et al., Improved cross-polarized radiation and wide impedance bandwidth from rectangular microstrip antenna with dumbbell-shaped defected patch surface. 2015. 15: p. 84-88.
[8] Firdausa, A., et al., Microstrip Antenna with a Defective Ground Structure (DGS) Motor for Wireless Fidelity Applications (Wi-Fi) at 2.4 GHz. 2024. 1(1): p. 13-17.
[9] Suganya, E., et al., Design and performance analysis of L-slotted MIMO antenna with improved isolation using defected ground structure for S-band satellite application. p. e5901.
[10] Zahid, M.N., et al., Design analysis of advanced power amplifiers for 5G wireless applications: a survey. 2024. 118(2): p. 199-217.

[11] Neto, A.G., et al., Compact Matryoshka DGS Using Dielectric Resonator. 2024.
[12] Arya, A.K., M.V. Kartikeyan, and A. Patnaik. Efficiency enhancement of microstrip patch antenna with defected ground structure. in 2008 International Conference on Recent Advances in Microwave Theory and Applications. 2008. IEEE.
[13] Lim, J., et al., Vertically periodic defected ground structure for planar transmission lines. 2002. 38(15): p. 1.
[14] Gour, S., A.J.T. Rathi, and R. Engineering, Earthen Lamp Shaped DGS Dual Band Microstrip Patch Antenna for High Return Loss in Biomedical Application. 2024.
[15] Sasirekha, D., et al. Design and bending analysis of wearable antenna with DGS based on PDMS substrate. in 2024 2nd International Conference on Networking and Communications (ICNWC). 2024. IEEE.
[16] Ismail, E., et al. Patch Antenna Design Using DGS Technique for Early Detection of Brain Tumor at Stages I to V. in 2024 6th International Youth Conference on Radio Electronics, Electrical and Power Engineering (REEPE). 2024. IEEE.
[17] Naik, K.K., et al., Design of flexible parasitic element patch antenna for biomedical application. 2020. 94: p. 143-153.
[18] Ahmad, S., et al., A wideband bear-shaped compact size implantable antenna for in-body communications. 2022. 12(6): p. 2859.
[19] Luo, L., et al., Compact dual-band antenna with slotted ground for implantable applications. 2019. 61(5): p. 1314-1319.
[20] Xu, L.-J., et al., Circularly polarized implantable antenna with improved impedance matching. 2020. 19(5): p. 876-880.
[21] Zhang, K., et al., Miniaturized Circularly Polarized Implantable Antenna for ISM-Band Biomedical Devices. 2017. 2017(1): p. 9750257.
[22] Liu, C., et al., Circularly polarized implantable antenna for 915 MHz ISM-band far-field wireless power transmission. 2018. 17(3): p. 373-376.